Luminescence from Collapsing Centimeter Bubbles Expanded by Chemical Reaction

Jérôme Duplat
Université Grenoble Alpes, INAC-SBT, F-38000 Grenoble, France CEA, INAC-SBT, F-38000 Grenoble, France

Emmanuel Villermaux
Aix Marseille Université, CNRS, Centrale Marseille, IRPHE UMR 7342, 13384 Marseille & Institut Universitaire de France, 75005 Paris, France

(Received 20 May 2014; revised manuscript received 2 March 2015; published 26 August 2015)

We report on a new method for realizing an exceptionally strong inertial confinement of a gas in a liquid: A centimetric spherical bubble filled with a reactive gaseous mixture in a liquid is expanded by an exothermic chemical reaction whose products condense in the liquid at the bubble wall. Hence, the cavity formed in this way is essentially empty as it collapses. The temperatures reached at maximum compression, inferred from the cavity radius dynamics and further confirmed by spectroscopic measurements exceed 20 000 K. Because the cavity is typically big, our findings also provide unique space and time resolved sequences of the events accompanying the collapse, notably the development of the inertial instability notoriously known to deter strong compression.

DOI: 10.1103/PhysRevLett.115.094501 PACS numbers: 78.60.Mq, 47.55.dd, 47.70.Fw, 47.70.Pq

The fate of an empty spherical cavity of radius $R_{\max}$ immersed in an infinite liquid bulk with density ρ at pressure P_{atm} is to collapse in a finite time [1] equal to $0.91R_{\max}\sqrt{\rho/P_{\mathrm{atm}}}$. The trajectory of the cavity radius $R(t)$, described by the Rayleigh-Plesset equation [2], shrinks to zero with a velocity diverging to infinity. Real voids in nature are, however, never strictly empty, but incorporate some vapor, either in equilibrium with the liquid, or from other incondensable constituents as in cavitation bubbles [3,4] and marine explosions [5]. As the cavity crunches and concentrates the liquid inertia on an ever smaller surface, the vapor is compressed at pressures and temperatures reaching appreciable levels. This *inertial confinement* process is at the origin of sonoluminescence [6,7], with temperatures up to a couple of 10^4 K, enough to ionize the gas in the cavity into a plasma, excite blackbody or bremsstrahlung radiation in the visible range [8,9], and is envisaged as a way to achieve nuclear fusion [10] of a deuterium-tritium mixture in several facilities around the world [11–13], with the aim of reaching up to 10^8 K. Here, we present a new way to achieve inertial confinement: A mixture of hydrogen and oxygen contained in a bubble in water is ignited, provoking the bubble expansion. The large (centimeters) cavity thus formed is nearly empty since most of the water vapor produced at the combustion stage condenses on the liquid bubble wall. Hence, high levels of compression are reached during cavity collapse. A rich phenomenology, including light emission at maximum compression, rebounds, bubble interface destabilization, and ultimate fragmentation is revealed by unique sequences resolved in space and time, allowing us, in particular, to measure destabilization wavelengths and growth rates.

A mixture of gaseous hydrogen and oxygen forming a bubble into a liquid is ignited. The chemical reaction,

$$\mathrm{H_2} + \frac{1}{2}\mathrm{O_2} \rightarrow \mathrm{H_2O} + \Delta H, \tag{1}$$

produces water plus several other compounds, like free radicals, in its vapor phase, with $\Delta H = -285$ kJ/mol, the formation enthalpy of water [14]. The released chemical energy causes pressure elevation inside the bubble, which first expands in the liquid, and collapses as water vapor condenses at the bubble wall.

Large, close-to-spherical bubbles of reactive mixtures are prepared according to two distinct protocols, depending on the viscosity of the liquid used: With water (density $\rho = 10^3$ kg/m^3, viscosity $\nu = 10^{-6}$ m^2/s), the nearly stoichiometric mixture is produced by the electrolysis of a 0.1M sodium hydroxide solution in a separate reservoir, with, however, a systematic excess of oxygen of order 5%–10%. The gas production reservoir is connected with the experimental tank ($10 \times 10 \times 20$ cm^3 wide, made of transparent glass), itself fitted on a free fall tower. A bubble injected at the tank base first raises towards the center of the tank whose vertical trajectory $z(t)$ is forced to undergo a free fall $z(t) = z_0 - \frac{1}{2}g(t - t_0)^2$ to compensate for gravity. Free fall lasts for 0.7 s, a time sufficient for the bubble to stabilize around a spherical shape. In glycerol (density $\rho = 1.26 \times 10^3$ kg/m^3, viscosity $\nu = 10^{-3}$ m^2/s), viscous stresses resist gravitational deformation of the bubble, which remains nearly spherical for about 1 s after injection at the base of the tank. The mixture is made from pure species stored in pressurized bottles and mixed at the desired ratio by precision flow meters. In both cases, when the bubble has attained its desired spherical shape, we shoot

a single pulse of a 195 mJ YAG-laser focalized at the center of the bubble, to ignite the mixture. Figure 1 illustrates how the bubble first expands, then collapses down to a minimum radius where its surface corrugates at the same time its core emits an intense light flash, then rebounds in a distorted shape, a prelude to its fragmentation. Figure 2 shows the evolution of the radii $R(t)$ of several bubbles with different initial volumes in water. After a short (less than a tenth of a millisecond) initial combustion phase, the bubble expands

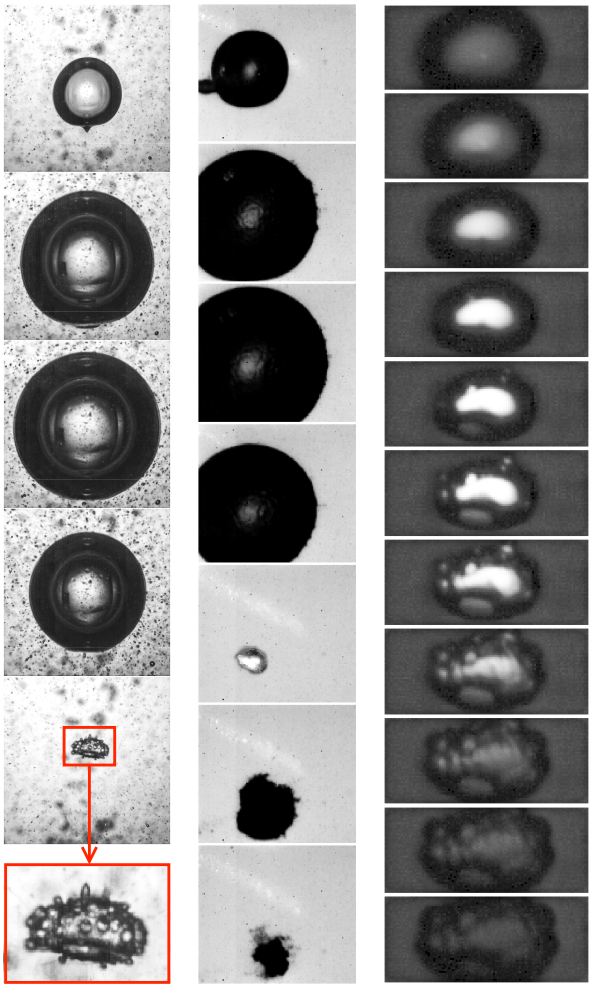

FIG. 1 (color online). Expansion and collapse dynamics of a stoichiometric hydrogen-oxygen mixture ignited in a bubble immersed in a liquid. (a) In glycerol, from ignition to maximal compression, by time steps of 0.7 ms. The width of the images is 3.3 cm. Closeup of the collapsed bubble 0.1 ms after maximal compression (image width 1 cm), showing interface destabilization. (b) In water, time steps of 0.45 ms from ignition, images width is 2 cm, showing a light flash at maximal compression, rebound, and fragmentation of the bubble. (c) Detailed dynamics around maximal compression, showing light emission, and interface destabilization. Glycerol, time step of 6.6 μs, image width 9.8 mm. (See the movies in the Supplemental Material for time resolved sequences.)

with some initial velocity $\dot{R}_0$, reaching its maximal radius $R_{\max}$ in a time $t_{\max}$ of the order of a millisecond. Trajectories are symmetric with respect to their maximum, and rescale when plotted against $(t - t_{\max})/\tau$ with $\tau = R_{\max}\sqrt{\rho/P_{\text{atm}}}$, expressing that the acceleration of the bubble interface $R(t)/\tau^2$ is the ratio of the force applied on the bubble $(P_{\text{atm}} - P)R(t)^2$ on the moving liquid mass $\rho R(t)^3$, if the cavity is empty (i.e., if its internal pressure P is zero). The rescaled trajectory is close to that anticipated for a strictly empty cavity, as seen in Fig. 2 comparing the real trajectory with the one obtained by integrating the Rayleigh-Plesset equation (surface tension is always negligible for these big bubbles) [1,2]

$$R\ddot{R} + \frac{3}{2}\dot{R}^2 + 4\nu\frac{\dot{R}}{R} = \frac{P - P_{\text{atm}}}{\rho}, \tag{2}$$

with $P = 0$. However, this solution is hardly distinguishable from other solutions with nonzero, small enough P. Assuming for instance that $P = P_0[R(t)/R_0]^{-3\gamma}$, with $\gamma = 7/5$ in order to represent the adiabatic expansion of a residual gas at pressure P_0 after the combustion phase, we obtain a compatible match with the experimental trajectory $R(t)$, as long as $P_0 < 2$ bars. Given that for a stoichiometric mixture at initial normal pressure ($P_{\text{atm}} = 1$ bar) and temperature ($T = 293$ K), the products of the reaction in a closed volume are at $T_c = 3500$ K and $P_c = 9.5$ bars [15]; the fact that $P_0 \ll P_c$ indicates that the water vapor produced by the reaction has necessarily condensed at the bubble wall into liquid water, soon after reaction completion.

After ignition, H_2 and O_2 burn according to Eq. (1) by propagating a flame from the ignition point, invading the bubble volume. During this combustion phase, lasting $\tau_c = R_0/c_f \approx 10^{-4}$ s with $c_f = 80$ m/s, the flame velocity at stoichiometry [16], the bubble pressure and temperature raise, at constant volume. The bubble is then composed of water vapor H_2O, free radicals like H· and OH·, remnants of

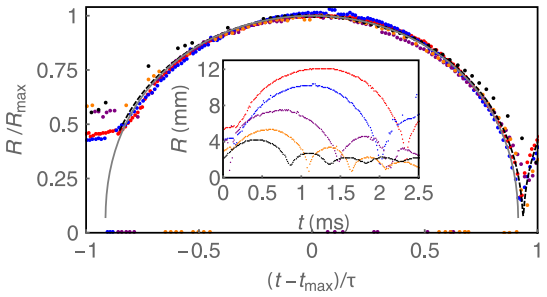

FIG. 2 (color online). Radius trajectories $R(t)$ for bubbles with several different radii R_0 in water (insert), and trajectories rescaled by their maximum $R_{\max}$, and time by $\tau = R_{\max}\sqrt{\rho/P_{\text{atm}}}$. Comparison with the solution of Eq. (2), with $P = 0$ (grey line) and $P = P_0[R(t)/R_0]^{-3\gamma}$, with $P_0/P_{\text{atm}} = 0.6$ (dashed line).

H_2 and O_2, to which we add traces of atomic H and O, and noncondensable species. Water vapor and the liquid water bulk are out of equilibrium, and the vapor condenses at the bubble wall, where its pressure is the saturation pressure $P_{\rm sat}$ at the liquid temperature (24 mbars at 293 K). The pressure difference $P_0 - P_{\rm sat} \approx P_0$ drives a flow at the bubble scale (clearly visible after ignition) of typical velocity $(P_0/\rho_g)^{1/2} = c_{\rm th} \approx 10^3$ m/s, the thermal velocity of the vapor molecules. The bubble interior is drained in a time $\tau_{\rm cond} = R_0/(\alpha c_{\rm th})$, of the order of 10^{-5} s for an accommodation coefficient α close to unity [17] at the bubble wall. This transport of the vapor from the core of the bubble to its wall is much more efficient than diffusion alone, which would require a time $\tau_{\rm diff} = R^2/D$ of the order of 1 s (with [15] $D = 10^{-4}$ m^2/s). Condensation competes with the bubble dynamics, whose typical time scale $\tau_{\rm dyn} = R/\dot{R}$ is itself a function of time. Thermodynamical equilibrium between the vapor and the liquid wall has time to establish as long as $\tau_{\rm cond} \ll \tau_{\rm dyn}$; otherwise the bubble dynamics occurs at frozen composition, a condition known to prevail a few nanoseconds prior to the maximal compression in collapsing sonoluminescence bubbles [18]. Despite the large size of our system, condensation is nearly complete at the beginning of the bubble expansion, since $R_0/\dot{R}_0 \approx 10^{-3}$ s, a time much larger than $\tau_{\rm cond}$. By removing the vapor from the mixture in the bubble, condensation also shifts the thermodynamical equilibrium, allowing for the chemical reaction to arrive almost at completion, raising higher the temperature up to $T_0 = 4400$ K for a residual pressure P_0 below 1 bar of dissociated compounds [15]. This explains why the bubble radius dynamics is such as if the bubble were empty.

A further proof of the condensation of the water vapor is provided by the comparison between the released chemical energy E_χ with the maximal mechanical energy E_m stored in the system. The latter is simply the work done by the pressure forces to expand the bubble up to its maximum radius $(4/3)\pi R_{\rm max}^3 P_{\rm atm}$, in absence of viscous dissipation (largely valid for water). The maximal chemical released energy is $E_\chi = -(2/3)[(4/3)\pi R_0^3/v_m]\Delta H$, where $v_m = \mathcal{R}T/P_{\rm atm}$ is the molar volume of the initial mixture at ambient pressure and temperature. The transformation efficiency of the chemical into mechanical energy $\eta = E_m/E_\chi$ is thus $\eta \approx 1.310^{-2}(R_{\rm max}/R_0)^3$, giving $\eta \approx 0.1$, independent of R_0 according to Figs. 1 and 2. This surprisingly weak value is also consistent with the initial dynamics of the radius trajectory $\dot{R}_0$. The maximal pressure reached during the combustion stage $P_c = 9.5$ bars is applied to the bubble wall during at most τ_c, after which condensation occurs on a short time scale, decreasing the pressure. Thu, from Eq. (2), we have $\dot{R}_0 \approx P_c\tau_c/(\rho R_0)$, an initial velocity of the order of 10 m/s. The kinetic energy communicated to the liquid bulk is $E_m = 2\pi\rho R_0^3\dot{R}_0^2$, so that the efficiency is expected to be $\eta \approx (v_m P_c^2)/(\rho c_f^2 \Delta H) \approx 0.1$. The quasi-instantaneous condensation of hot water vapor at the bubble wall prevents the pressure reached during the combustion stage to fully transfer the available chemical energy into mechanical motion. A large fraction of this energy is transferred to the liquid bulk as heat by condensation.

Close to the final collapse and as soon as $\tau_{\rm dyn}$ becomes the smallest time scale (as $\dot{R}$ diverges), the composition of the bubble is frozen, and remain free radicals, possible excesses of H_2 or O_2 if the mixture is not perfectly stoichiometric, and traces of inert incondensables. The compression of these remnants ultimately balances liquid inertia, and the bubble interface decelerates, then rebounds violently, as seen in Figs. 1(c) and 3. From the recorded trajectory $R(t)$ in glycerol (see Fig. 3), one identifies the rebound time $t_\star$, measures the acceleration $\ddot{R}(t_\star)$, and computes the pressure in the bubble from Eq. (2) as $P(t_\star) = \rho R(t_\star)\ddot{R}(t_\star) + P_{\rm atm}$. With $\ddot{R}(t_\star) = 1.2 \times 10^6$ m/s^2 for the trajectory in Fig. 1(c), we have $P(t_\star) = 36$ bars. The temperature, assuming an adiabatic compression close to $t_\star$ as long as water vapor does not dissociate [19], is $T(t_\star) = T_0[R_0/R(t_\star)]^{3(\gamma-1)}$ with $\gamma = 7/5$. With $T_0 = 4400$ K, we expect $T(t_\star) = 12900$ K.

Since $\ddot{R} > 0$ at rebound, the interface acceleration (and the pressure gradient at the interface) is oriented from the light interior towards the heavy liquid, making the interface unstable in the sense of Rayleigh and Taylor [20]. The instability development is imaged in real time in Fig. 1(c). The viscous limit of this instability suits to very large accelerations, for which viscosity ultimately limits mode selection, and controls its growth rate [20–24]. The instability wavelength λ, estimated from the maximal acceleration $\ddot{R}(t_\star)$, is about $\lambda \approx 20[\nu^2/\ddot{R}(t_\star)]^{1/3}$, and the amplification rate is $\omega \approx 0.5[\ddot{R}(t_\star)^2/\nu]^{1/3}$. In glycerol (the gas viscosity is comparatively negligible), this provides $\lambda \approx 2$ mm, of the order of the distance between the protrusions visible at the bubble surface in Fig. 1(c). The net growth of the instability during the rebound time is $\exp[\omega(R(t_\star)/\ddot{R}(t_\star))^{1/2}] \approx 2.7$, a moderate net gain explaining why the bubble has not disjointed at rebound but amplified weak, yet visible corrugations. In water, from

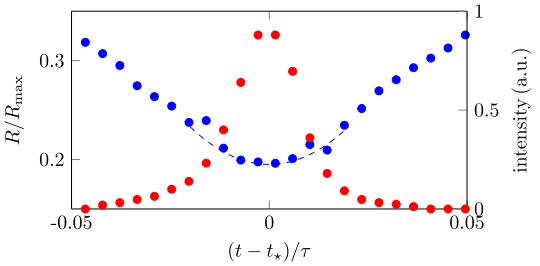

FIG. 3 (color online). Blue dots: Bubble radius close to its minimum [corresponding to Fig. 1(c)], at the maximum compression time $t_\star$, as the trajectory rebounds. Dashed line: Parabolas $R(t) = R(t_\star) + \ddot{R}(t_\star)[t-t_\star]^2/2$. Red dots: Luminance of the flash (a.u.). $\tau = 1.5$ ms.

the radius trajectory in Fig. 2 with $R_{\max} = 1.2$ cm (in red), the rebound is best fitted by the Rayleigh-Plesset equation in Eq. (2) for $P_0 = 0.6$ bars assuming a final adiabatic compression with $\gamma = 7/5$. This predicts $P(t_\star) = 850$ bars, $R(t_\star) = 0.08R_{\max}$, and an acceleration at rebound $\ddot{R}(t_\star) = 8.8 \times 10^7$ m/s^2. The instability net gain is now extremely large, consistent with the observation that the bubble fragments at collapse [Fig. 1(b)].

Close to maximal compression, the bubble interior emits a light flash, visible in Figs. 1 and 3. The spectral analysis of this flash with bubbles in water provides further information when compared to that of the initial flame in the combustion stage. The emitted light is reflected on a 400 lines/mm diffraction grating. The camera exposure time is large compared to the flash duration, so that all the flash energy is collected in only one frame, and is clearly distinct from the combustion stage. During combustion, the temperature is $T_f = 3500$ K and two broad peaks (or bands, see Fig. 4) are observed in the range 570–630 nm. The first one is centered around the 590 nm atomic sodium double ray [25]. The live spectrum was recorded without slit due to the weakness of the source, yielding broadening of the spectral lines, but a resolved spectral analysis of the flame with the same mixture performed in a separate closed reactor identified undoubtedly the double ray of sodium, present in traces and enhanced in the spectrum at high pressure [26,27]. A second broader band is centered around 620 nm, characteristic of the emission spectrum of water vapor [28,29]. During the flash however, only the sodium peak is visible, with an intensity reduced by a factor 3 compared to the combustion stage. The absence of the water vapor emission band suggests that the vapor has condensed at the bubble wall.

The comparison of the spectra in Fig. 4 gives an estimation of the temperature T_f of the flash: The luminance I is proportional to the total number of emissive sodium particles N, the duration of the light emission τ_e and to a Boltzmann prefactor

$$I \propto N\tau_e \exp\left(-\frac{T^*}{T}\right), \tag{3}$$

where $T^* = 24\,400$ K is the temperature (energy) level of the exited $3p$ atomic state [25]. The combustion period is long compared to the camera exposure time which therefore limits the emission time to $\tau_{e,c} = 50$ μs. The flash occurs at the maximal compression and has a shorter duration, given by the rebound time [see Fig. 1(c)] so that $\tau_{e,f}/\tau_{e,c} \approx 1/6$. If there are N_c sodium atoms trapped in the cavity after the combustion stage, and given their affinity for liquid water, a conservative estimate of their number N_f at the flash is that their concentration remains constant, that is $N_f/N_c \approx [R(t_\star)/R_0]^3 \approx 1/200$. Since the temperature of the remnant gas in the cavity at maximum light emission is such that

$$\frac{I_f}{I_c} = \frac{N_f}{N_c}\frac{\tau_{e,f}}{\tau_{e,c}} \exp\left(\frac{T^*}{T_c} - \frac{T^*}{T_f}\right) \tag{4}$$

and since $I_f/I_c = 1/3$ from Fig. 4, we have $T_f = 26\,000$ K, and order of magnitude consistent with the one obtained from the fit of the radius trajectory in Fig. 2 (in red) by the Rayleigh-Plesset equation in Eq. (2), ignoring the endothermic dissociation of water at high temperature, and predicting $T_f = 29\,900$ K.

While micronic sonoluminescent bubbles emit pulses of light lasting for a few hundreds of picoseconds and millimetric cavitation bubbles flash for nanoseconds [4,30], we have shown that during the space and time resolved collapse of a centimetric cavity, light emission lasts for tens of microseconds. The benefit of the present method is to upscale the phenomena making them bigger [31,32], longer, and therefore easier to document, offering a unique experimental benchmark for the development of the inertial instability deterring strong compression at collapse [13,33]. A bubble expanded by an exothermic reaction producing condensable products is also a way to enhance the collapse strength, precisely because the cavity is essentially empty.

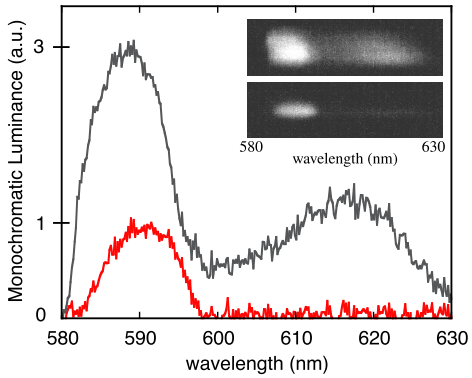

FIG. 4 (color online). Spectral content (wavelength in nanometers) of the light emitted during the combustion stage (black), and during the flash (red) maximal bubble compression, integrated for a time $\tau_e = 50$ μs. Inserts: Raw snapshots of the flame (top) and of the flash (bottom) as recorded behind a grating.

[1] L. Rayleigh, Philos. Mag. **34**, 94 (1917).
[2] M. S. Plesset and A. Prosperetti, Annu. Rev. Fluid Mech. **9**, 145 (1977).
[3] E. Meyer and H. Kuttruff, Z. Angew. Phys. **11**, 325 (1959).
[4] C. D. Ohl, O. Lindau, and W. Lauterborn, Phys. Rev. Lett. **80**, 393 (1998).
[5] R. H. Cole, *Underwater Explosions* (Princeton University Press, Princeton, New Jersey, 1948).
[6] M. P. Brenner, S. Hilgenfeldt, and D. Lohse, Rev. Mod. Phys. **74**, 425 (2002).

[7] D. J. Flannigan and K. S. Suslick, Nature (London) **434**, 52 (2005).
[8] R. Hiller, S. Putterman, and B. P. Barber, J. Acoust. Soc. Am. **92**, 2454 (1992).
[9] D. J. Flannigan and K. S. Suslick, Nat. Phys. **6**, 598 (2010).
[10] S. Atzeni and J. Meyer-Ter-Vehn, *The Physics of Inertial Fusion*, International Series of Monographs on Physics, Vol. 125 (Clarendon Press, Oxford, 2004).
[11] P. A. Holstein *et al.*, Laser Part. Beams **17**, 403 (1999).
[12] J. D. Lindl *et al.*, Nucl. Fusion **51**, 094024 (2011).
[13] O. A. Hurricane *et al.*, Nature (London) **506**, 343 (2014).
[14] D. R. Lide, *CRC Handbook of Chemistry and Physics* (CRC Press, Boca Raton, FL, 2004).
[15] C. Morley, Gaseq, http://www.gaseq.co.uk, 2005.
[16] D. A. Senior, Combust. Flame **5**, 7 (1961).
[17] P. Davidovits *et al.*, Geophys. Res. Lett. **31**, L22111 (2004).
[18] B. D. Storey and A. J. Szeri, J. Fluid Mech. **396**, 203 (1999).
[19] B. D. Storey and A. J. Szeri, Proc. R. Soc. A **456**, 1685 (2000).
[20] S. Chandrasekhar, *Hydrodynamic and Hydromagnetic Stability* (Dover, New York, 1961).
[21] See Supplemental Material at http://link.aps.org/supplemental/10.1103/PhysRevLett.115.094501 for the viscous corrections to the Rayleigh-Taylor instability, and time-resolved sequences of the phenomenon.
[22] M. S. Plesset, J. Appl. Phys. **25**, 96 (1954).
[23] M. S. Plesset, Phys. Fluids **17**, 1 (1974).
[24] R. Menikoff, R. C. Mjolsness, D. H. Sharp, and C. Zemach, Phys. Fluids **20**, 2000 (1977).
[25] A. Kramida, Y. Ralchenko, J. Reader, and N. A. Team, *NIST Atomic Spectra Database*, Ver. 5.1 (National Institute of Standards and Technology, Gaithersburg, MD, 2013), http://physics.nist.gov/asd.
[26] T. V. Gordeychuk and M. V. Kazachek, in *Nonlinear Acoustics Fundamentals and Applications*, edited by B. O. Enflo, C. M. Hedberg, and L. Kari, AIP Conference Proceedings, Vol. 1022, (AIP, New York, 2008), pp. 201–204.
[27] H. C. Chu, S. Vo, and G. A. Williams, Phys. Rev. Lett. **102**, 204301 (2009).
[28] T. Kitagawa, Proc. Imp. Acad. (Tokyo) **12**, 281 (1936).
[29] A. G. Gaydon, Proc. R. Soc. A **181**, 197 (1942).
[30] B. Kappus, S. Khalid, and S. Putterman, Phys. Rev. E **83**, 056304 (2011).
[31] H. M. Müller, Acta Acustica **16**, 22 (1966).
[32] D. Lohse, Nature (London) **392**, 21 (1998).
[33] V. A. Smalyuk *et al.*, Phys. Rev. Lett. **112**, 185003 (2014).